REPORT DOCUMENTATION PAGE

Form Approved OMB No. 0704-0188

1. REPORT DATE *(DD-MM-YYYY)*	2. REPORT TYPE	3. DATES COVERED *(From – To)*
07-05-2010	Final Report	15 September 2008 - 15-Sep-09

4. TITLE AND SUBTITLE

Evaluation of terahertz quantum cascade laser sources as a potential portable non-destructive evaluation method for the inspection of aircraft structures

5a. CONTRACT NUMBER
FA8655-08-1-3090

5b. GRANT NUMBER

5c. PROGRAM ELEMENT NUMBER

6. AUTHOR(S)

Professor Harvey E Beere

5d. PROJECT NUMBER

5d. TASK NUMBER

5e. WORK UNIT NUMBER

7. PERFORMING ORGANIZATION NAME(S) AND ADDRESS(ES)
University of Cambridge
Cavendish Laboratory
Cambridge Cb3 0HE
United Kingdom

8. PERFORMING ORGANIZATION REPORT NUMBER

N/A

9. SPONSORING/MONITORING AGENCY NAME(S) AND ADDRESS(ES)

EOARD
Unit 4515 BOX 14
APO AE 09421

10. SPONSOR/MONITOR'S ACRONYM(S)

11. SPONSOR/MONITOR'S REPORT NUMBER(S)
Grant 08-3090

12. DISTRIBUTION/AVAILABILITY STATEMENT

Approved for public release; distribution is unlimited.

13. SUPPLEMENTARY NOTES

14. ABSTRACT

This report results from a contract tasking University of Cambridge as follows: Description of Work: The first phase of the project aims to reproduce the performance figures from the reference THz QCL design [3]. To achieve high temperature operation the device utilises a double-metal (DM) waveguide. This utilises a novel gold-to-gold thermal compression wafer bonding technique that has been developed at the Cavendish Laboratory which incorporates a self-aligned dry etch process.Standard electrical (I-V) and lasing emission (L-I, L-f, L-T, electroluminescence) characterisation will be taken and compared with the simulation data. Following validation of the USAF modelling code the first LO phonon injection design will be fabricated. The design aims to directly inject electrons into the upper state of the lasing transition through an LO phonon transition; with the aim of preserving the upper state lifetime at elevated temperatures Again standard characterisation of this device in a DM waveguide will be performed. Depending on the promise of this design philosophy further iterative improvements will be scheduled. If the above device shows significantly degraded performance an alternative design approach will be adopted.

15. SUBJECT TERMS
EOARD, Semiconductors, semiconductor lasers, terahertz technology

16. SECURITY CLASSIFICATION OF:			17. LIMITATION OF ABSTRACT	18, NUMBER OF PAGES	19a. NAME OF RESPONSIBLE PERSON
a. REPORT	**b. ABSTRACT**	**c. THIS PAGE**	UL	9	A. GAVRIELIDES
UNCLAS	UNCLAS	UNCLAS			**19b. TELEPHONE NUMBER** *(Include area code)* +44 (0)1895 616205

Standard Form 298 (Rev. 8/98)
Prescribed by ANSI Std. Z39-18

Table of Contents:

List of Figures:

*Fig 1: Band diagram of three periods of the USAF's 2.5THz resonant phonon injection and depletion active region, under an applied electric field of 13.5kV/cm. The moduli squared wavefunctions of the upper state (red) and lower (blue) lasing states are shown. Also highlighted are the two states associated with resonant LO phonon injection/depopulation (green/black). The layer thicknesses in Angstroms for this 3-well per period design are **30**/94/**25**/72/**45**/154 (Al$_{0.15}$Ga$_{0.85}$As barriers in bold).*

*Fig 2: Diagram shows 3-periods of the 3-well design biased at 13kV/cm. The moduli squared wavefunctions of the upper lasing state (red) and lower (blue) lasing states are shown. Layers in Angstroms (starting with largest phonon injection well): 150/**18**/90/**40**/73/**45**. Silicon doping in the 73Å well was 4x10^{16}cm^{-3} to produce a sheet density of ~3x10^{10}cm^{-2} per module.*

Fig 3: High resolution X-ray diffraction curve of the wafer growth of the 2.2THz USAF resonant intra-well direct LO Phonon THz QCL structure (V624). The black curve shows the as-grown wafer structure, whereas the red curve shows a simulation for the design structure; corresponding to a 0.24% thinner active region.

Fig 4: Voltage vs current density (V/J) and light output power vs current density (L/J) curves from a 3.00mm x 0.25mm ridge laser (single plasmon waveguide architecture) from the 2.2THz USAF wafer, V624. The laser was operated in pulsed mode with 250ns long pulses at a repetition rate of 80kHz.

Fig 5: Voltage vs current density (V/J) and light output power vs current density (L/J) curves from a 3.00mm x 0.25mm ridge laser (single plasmon waveguide architecture) from the 2.2THz USAF wafer, V624. The laser was operated in pulsed mode with 250ns long pulses at a repetition rate of 80kHz.

Fig 6: Voltage vs current density (V/J) and light output power vs current density (L/J) curves from a 3.00mm x 0.1mm ridge laser (single plasmon waveguide architecture) from the 3.0THz MIT Reference wafer, V569 (device 5). The laser was operated in pulsed mode with 250ns long pulses at a repetition rate of 80kHz.

Fig 7: Voltage vs current density (V/J) and light output power vs current density (L/J) curves from a 1.50mm x 0.2mm ridge laser (single plasmon waveguide architecture) from the 2.5THz USAF wafer, V585 (device 13). The laser was operated in pulsed mode with 250ns long pulses at a repetition rate of 80kHz.

Summary of fourth quarter's progress (Sep 09 – Dec 09):

● Growth of the new 2.2THz USAF design.

● Fabrication and assessment of the LO-Phonon THz QCL design.

Introduction and Methodology

This project aims to increase the operating temperature of one of the best performing THz QCL designs to date [1]. The proposed designs came from a series of interesting results that was initially noted when coupling a very simple 4-well per period QCL model with a genetic algorithm; which is similar to successfully demonstrated resonant-phonon THz QCL designs. Phase one of the project was to; (a) replicate the 3THz MIT resonant LO Phonon QCL structure, as a reference baseline and then (b) fabricate a 2.5THZ USAF direct LO-Phonon injection QCL design. This would allow better relative comparison of the performance of the USAF design, since it is well know that the ultimate temperature performance of the laser structure is very sensitive to doping levels in the injector region [2] and the use of Cu-Cu (instead of Au-Au) as a thermo-compression bond in the metal-metal waveguide fabrication [3]. Although, the Au-Au thermo-compression bond tends to produce a reduction in temperature performance in comparison to a Cu-Cu bond (by ~10-15K), it is a more reliable and stable process. Phase two of the project would build on the results of phase one or explore alternative design strategies.

As part of a standard characterisation programme, all grown THz QCL wafers would be assessed using high resolution X-ray diffraction, to determine both crystalline quality and the thickness of the laser active region. They would then be processed into both single plasmon ridge waveguide lasers (1.5-3mm long and 0.1-0.2mm wide) and metal-metal waveguide lasers (1-2mm long and 0.05-0.08mm wide). For electrical and optical characterisation, devices are indium soldered onto copper holders and mounted on the cold finger of a continuous flow liquid Helium cryostat. Electrical measurements were made in a two terminal configuration. The light output power measurements were measured under vacuum with a broad area thermopile detector mounted on the cryostat window at a distance ~1mm from the laser facet. Lasing emission spectra are taken using a Bruker IFS66v/s Fourier Transform Infrared (FTIR) spectrometer with 7.5GHz resolution.

Following the successful reproduction of the reference structure in Q1/Q2, it was shown in Q2/Q3 that although the first 2.5THz QCL showed promising electrical characteristics, i.e. the device operated in the correct voltage regime and passed currents of the expected order, with no unexpected breaks (i.e. field mis-alignment) at low biases, the structure did not optically lase. This was confirmed in the low temperature differential resistance trace (dV/dI) showing no significant features. In discussion with the design team at USAF it was decided that the second phase of this project (Q3/Q4), would investigate a new direct LO-Phonon injection device design.

Results and Discussion

In the coherent (delocalized) wavefunction picture, the injection mechanism in THz QCLs is dominated at low temperatures by carrier-carrier scattering. The radiative states are in the form of an anticrossed "doublet" and the depopulation mechanism is a near-resonant phonon transition to the next period. Since thicker barriers are used in both the injection and extraction processes, resonant tunneling is assumed to play a large role in transferring current between. Since it is difficult to increase this desired scattering rate without also increasing parasitic (leakage) channels it appeared that further improvements should concentrate on injection mechanisms which show a smaller parasitic dependence.

The first USAF design from the genetic algorithm indicated that direct electron injection into the upper lasing state, using a near-resonant phonon transition, could be an efficient solution. The simplest way to achieve this was to remove one of the wells in the MIT reference LO phonon design and then to reduce the injection barrier in an attempt to delocalized the upper state enough to receive the phonon scattering from the previous period. In this design the direct phonon injection mechanism was an inter-well process, figure 1.
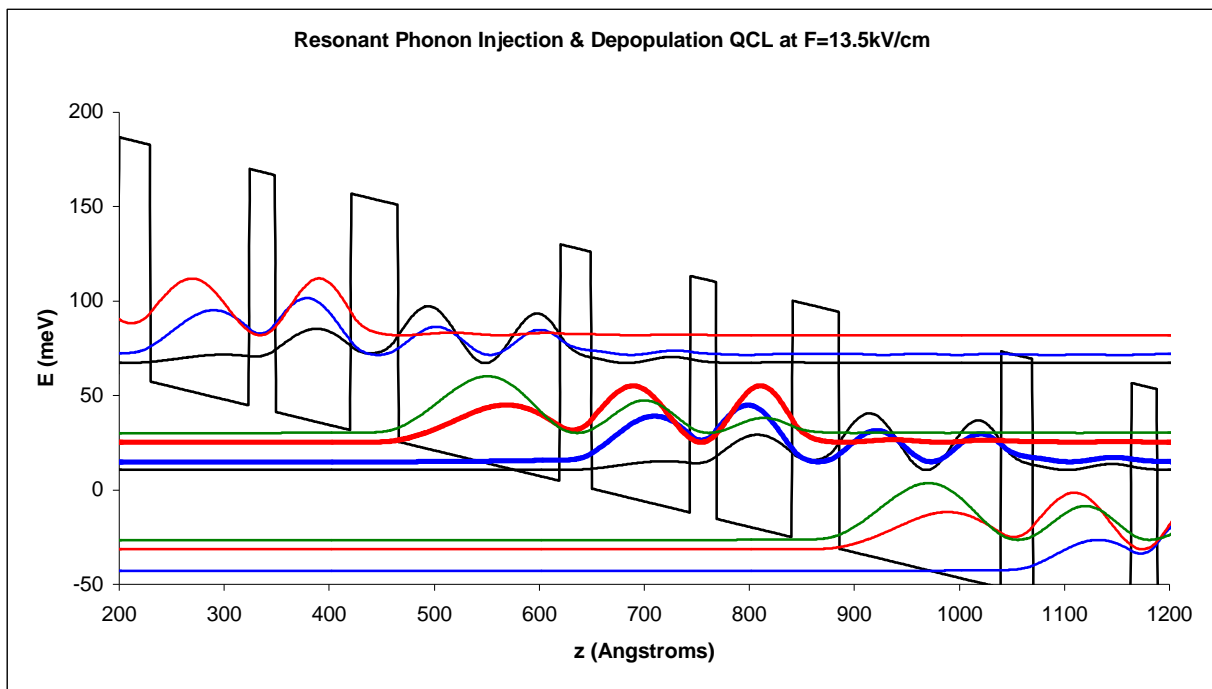
Fig 1: Band diagram of three periods of the USAF's 2.5THz resonant phonon injection and depletion active region, under an applied electric field of 13.5kV/cm. The moduli squared wavefunctions of the upper state (red) and lower (blue) lasing states are shown. Also highlighted are the two states associated with resonant LO phonon injection/depopulation (green/black). The layer thicknesses in Angstroms for this 3-well per period design are $30/94/25/72/45/154$ ($Al_{0.15}Ga_{0.85}As$ barriers in bold).

An alternative approach to achieve direct phonon injection into the upper lasing state is to use an intra-well process. The design still aimed to utilise a 3-well per period approach as per the first design so once again minor adjustments to the barrier thicknesses were necessary to bring the states back to a configuration/overlap similar to the reference MIT design, figure 2. This resulted in a small frequency shift of the lasing states to 9.1meV or ~2.2THz, at an alignment field of F=13.0kV/cm.
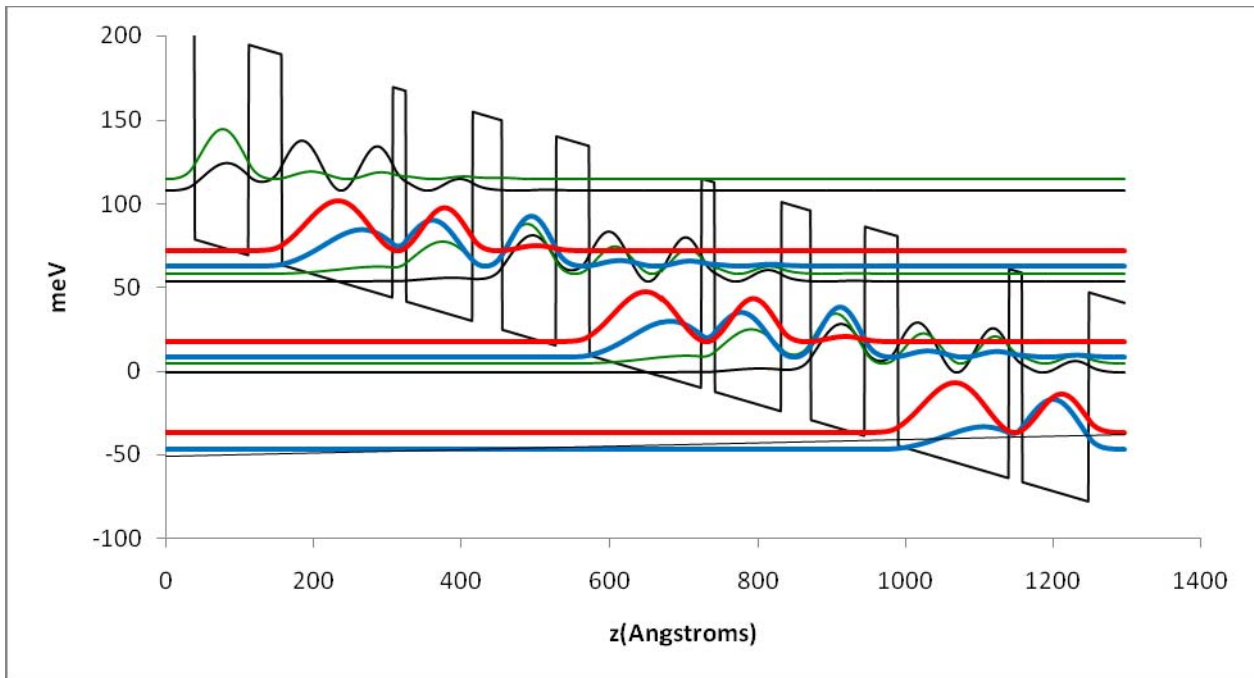
*Fig 2: Diagram shows 3-periods of the 3-well design biased at 13kV/cm. The moduli squared wavefunctions of the upper lasing state (red) and lower (blue) lasing states are shown. Layers in Angstroms (starting with largest phonon injection well): 150/**18**/90/**40**/73/**45**. Silicon doping in the 73Å well was $4x10^{16}cm^{-3}$ to produce a sheet density of $\sim3x10^{10}cm^{-2}$ per module.*

The high resolution x-ray diffraction scans from the grown structure (V624) confirms the accuracy of growth of the as-requested THz QCL design. For comparison figures 3 (top) and 3 (bottom) show the high resolution X-ray diffraction curve (black trace) for the 2.2THz THZ QCL grown wafer (V624), as well as a simulation of the AR for this structure (red trace). Both the large angle scan (figure 2a) and the expanded view of the fifth, six and seventh order satellite peaks (figure 2b) shows that the as grown active region is within the 1% thickness tolerance generally required. Furthermore the intensity and linewidths (~20 arc.sec) of the higher order satellite peaks confirm the high quality of MBE growth achieved.
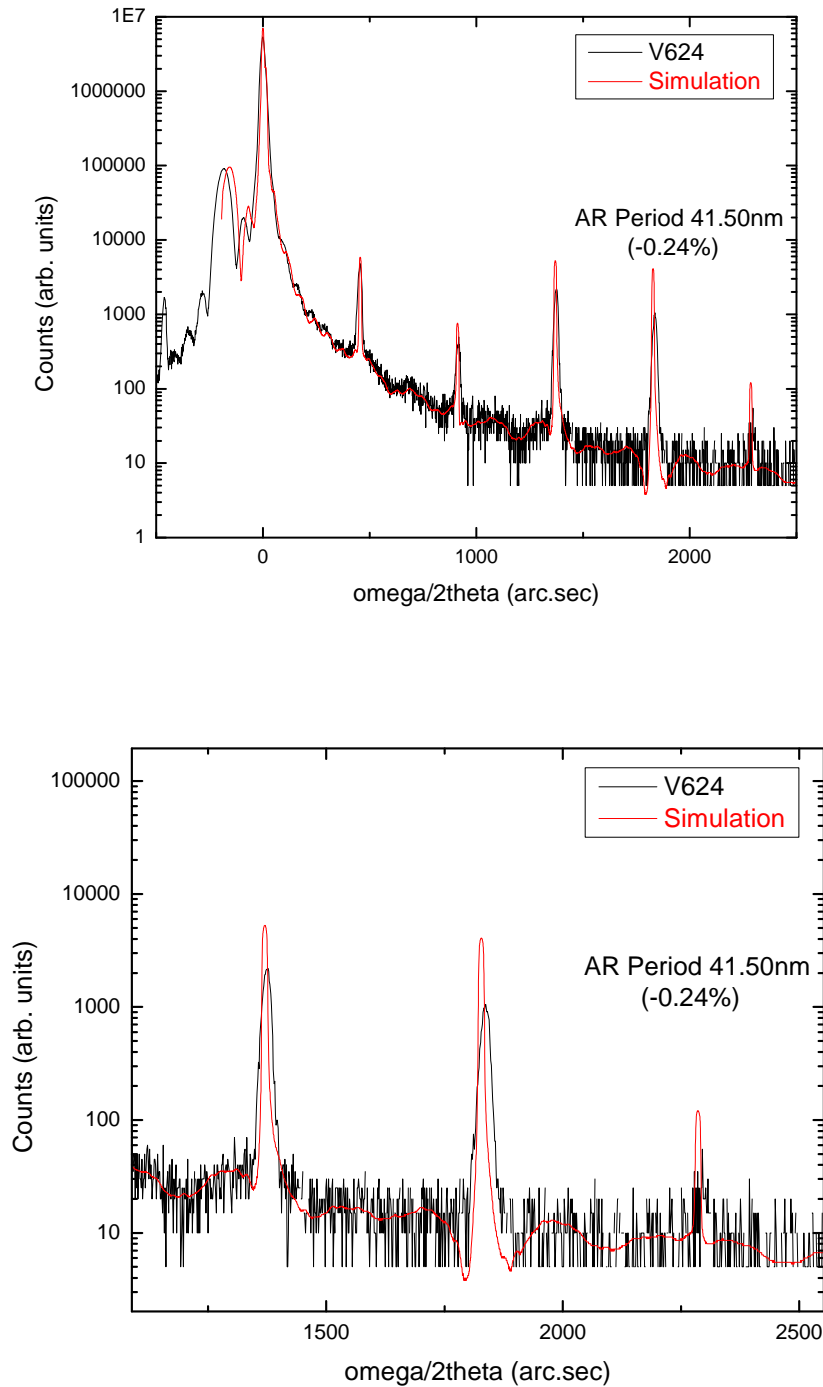
Fig 3: High resolution X-ray diffraction curve of the wafer growth of the 2.2THz USAF resonant intra-well direct LO Phonon THz QCL structure (V624). The black curve shows the as-grown wafer structure, whereas the red curve shows a simulation for the design structure; corresponding to a 0.24% thinner active region.

The electrical transport through a 3.0mm x 0.25mm single plasmon device from sample V624 (device 8) unfortunately does not show the three distinct different transport regimes associated with THz QCLs, figure 3; (a) initially the device is resistive, (b) at the onset of band alignment lasing takes place, this is marked by the sharp 'knee' feature, (c) under progressively higher applied electric fields the breaking of band alignment. At 4K, the laser ridge shows characteristics only associated with typical below threshold alignment IVs; however no lasing in the structures was observed. Worryingly the intra-well design structure appears to suffer from significant parasitic

leakage channels at low fields. Both of these features are confirmed by the differential resistance trace (dV/dI) in the insert, which shows (a) no step discontinuity signature for lasing at the expected alignment field and (b) no low bias high resistive channel characteristics. On a positive note the device operates in the correct voltage regime and passes currents of the expected order, without unexpectedly breaking (band mis-alignment) at low biases (fields).
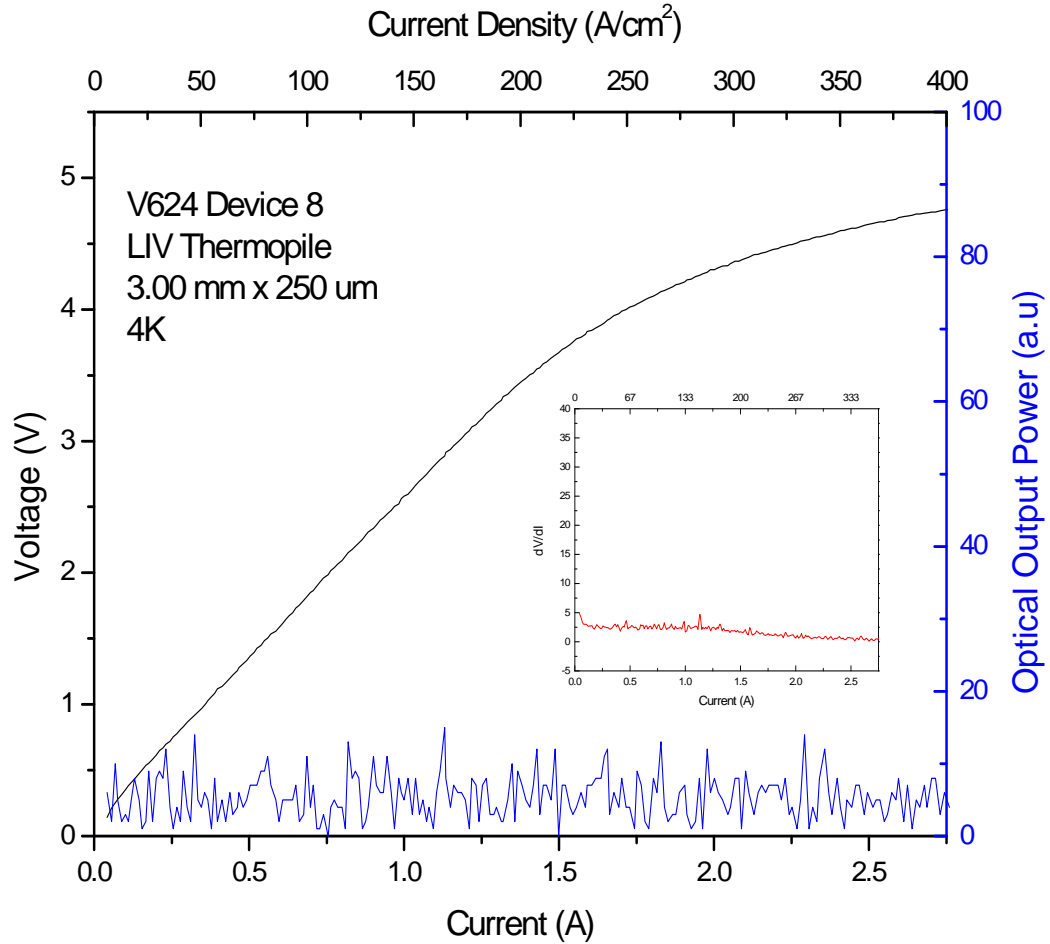

Fig 4: Voltage vs current density (V/J) and light output power vs current density (L/J) curves from a 3.00mm x 0.25mm ridge laser (single plasmon waveguide architecture) from the 2.2THz USAF wafer, V624. The laser was operated in pulsed mode with 250ns long pulses at a repetition rate of 80kHz.

As with all the previous USAF THz QCL designs multiple ridge lasers were tested from at least two processing runs to ensure that the above results are not a consequence of a poor processing run, see figure 4 below. As before the electrical transport through a 3.0mm x 0.25mm single plasmon device from sample V624 (device 10) did not lase.
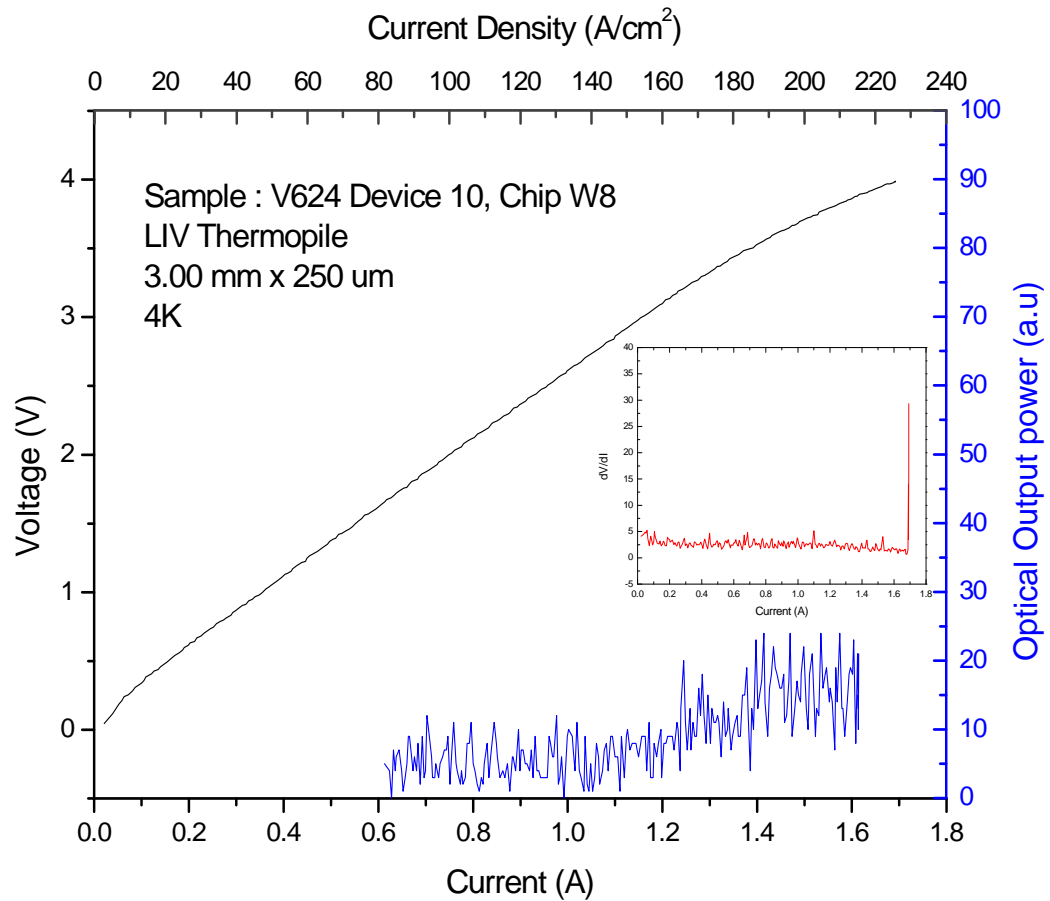
Fig 5: Voltage vs current density (V/J) and light output power vs current density (L/J) curves from a 3.00mm x 0.25mm ridge laser (single plasmon waveguide architecture) from the 2.2THz USAF wafer, V624. The laser was operated in pulsed mode with 250ns long pulses at a repetition rate of 80kHz.

For comparison the electrical characteristics from the 3.0THz MIT Reference structure (V569) and the 2.5THz USAF QCL (V585) are presented in figure 6 and figure 7, respectively. With each design, at very low fields the device is initially highly resistive;. which can be seen in the high values of dV/dI at low currents. This suggests that the new 2.2THz THz QCL design suffers from large parasitic current leakage channels, which will significantly compromise the performance of the laser. From previous experience it is unlikely that the design will lase, even when processed into a double metal waveguide.
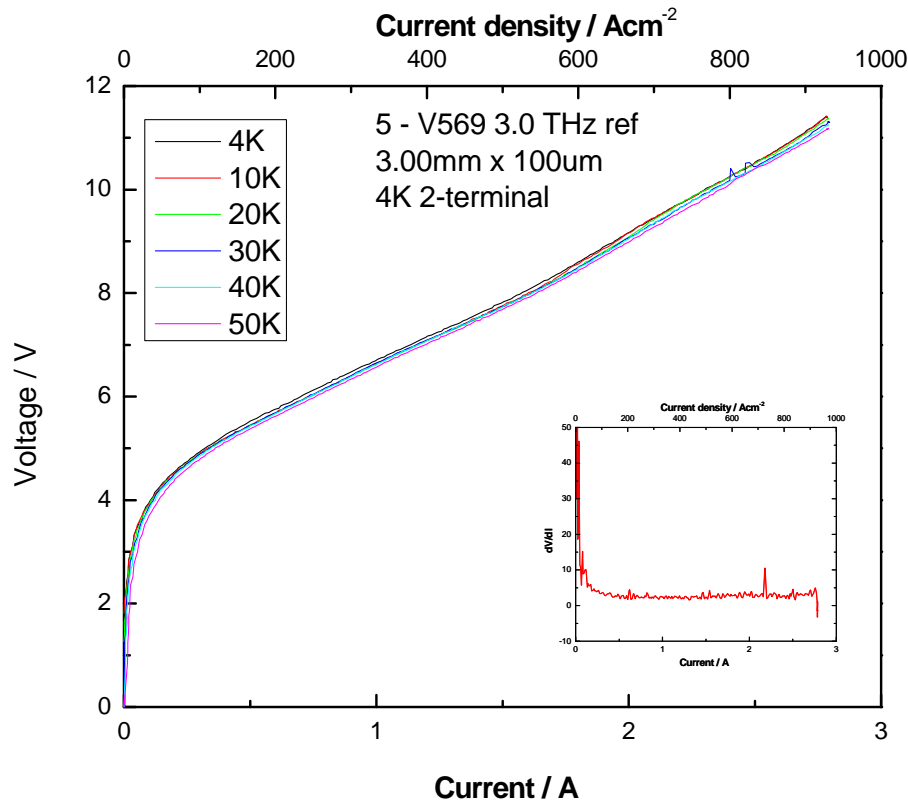
Fig 6: Voltage vs current density (V/J) and light output power vs current density (L/J) curves from a 3.00mm x 0.1mm ridge laser (single plasmon waveguide architecture) from the 3.0THz MIT Reference wafer, V569 (device 5). The laser was operated in pulsed mode with 250ns long pulses at a repetition rate of 80kHz.
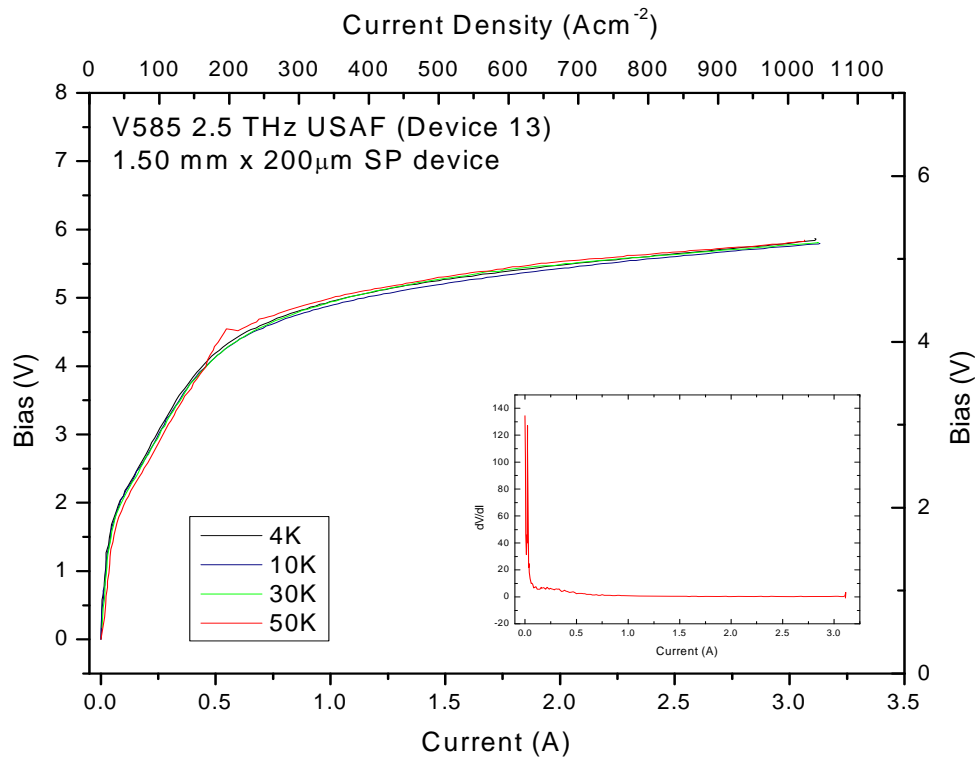

Fig 7: Voltage vs current density (V/J) and light output power vs current density (L/J) curves from a 1.50mm x 0.2mm ridge laser (single plasmon waveguide architecture) from the 2.5THz USAF wafer, V585 (device 13). The laser was operated in pulsed mode with 250ns long pulses at a repetition rate of 80kHz.

Conclusions and Future Work

The absence of THz lasing from both of the USAF 2.2THz and 2.5THz direct phonon injection QCL designs highlights the importance and challenges of THz QCL design to achieve (a) efficient population of carriers into the upper lasing state, (b) efficient depopulation of the lower lasing state, with (c) optimal carrier transport through the structure. By effectively removing the influence of the injection barrier from the design, by reducing this barrier sufficiently to allow the upper state to be delocalized enough to receive phonon scattering from the previous period, parasitic scattering of carriers out of the upper state may have compromised the success of this design strategy. However the initial design premise was an interesting one and a novel approach at increasing the maximum operating temperature of this new type of laser.

References

[1] B. Williams, *et al.,* Optics Express **13(9)**, 3331 (2005)
[2] H. Liu, *et al.*, Appl. Phys. Lett. **87**, 141102 (2005)
[3] M. Belkin, *et al.,* Optics Express **16(5)**, 3242 (2008)

List of Symbols, Abbreviations, and Acronyms

THz	Terahertz (10^{12} Hz)
QCL	Quantum Cascade Laser
MIT	Massachusetts Institute of Technology
USAF	AFRL/RXPS Design Team; Program Manager C. Stutz
LO-Phonon	Longitudinal Optical Phonon
MBE	Molecular beam epitaxy
AR	Active region
V	Voltage
J	Current density
L	Light output
J_{max}	Maximum lasing current density (before laser ceases to operate)
J_{th}	Current density at lasing threshold
FTIR	Fourier Transform Infrared

Disclosure of Invention

I, Dr Harvey Beere, certify that there were no subject inventions to declare during the performance of this grant.